

A Novel Portable Absolute Transient Hot-Wire Instrument for the Measurement of the Thermal Conductivity of Solids

Marc J. Assael¹, Konstantinos D. Antoniadis¹,
Ifigeneia N. Metaxa¹, Sofia K. Mylona¹,
John-Alexander M. Assael^{2,3}, Jiangtao Wu⁴,
Miaomiao Hu⁵

Abstract A new portable absolute Transient Hot-Wire instrument for measuring the thermal conductivity of solids over a range of 0.2 to 4 Wm⁻¹K⁻¹ is presented. The new instrument is characterized by three novelties: a) an innovative two-wires sensor which provides robustness and portability, while at the same time employs a soft silicone layer to eliminate the effect of the contact resistance between the wires and the sample, b) a newly designed, compact portable printed electronic board employing an FPGA architecture CPU to the control output voltage and data processing - the new board replaces the traditional, large in size Wheatstone-type bridge system required to perform the experimental measurements, and c) a cutting-edge software suite, developed for the mesh describing the structure of the sensor, and utilizing the Finite Elements Method to model the heat flow. The estimation of thermal conductivity is modeled as a minimization problem and is solved using Bayesian Optimization. Our revolutionizing proposed methodology exhibits radical speedups of up to 120x, compared to previous approaches, and considerably reduces the number of simulations performed, achieving convergence only in a few minutes. The new instrument was successfully employed to measure, at room temperature, the thermal conductivity of, two thermal conductivity reference materials,

Marc J. Assael
assael@auth.gr

- ¹ Laboratory of Thermophysical Properties & Environmental Processes, Chemical Engineering Department, Aristotle University, Thessaloniki 54636, Greece
- ² Tessera Multimedia, Dardanellion 11, 57010 Pefka, Thessaloniki, Greece
- ³ Department of Computer Science, University of Oxford, Oxford OX1 3QD, UK
- ⁴ Center of Thermal and Fluid Science, Xi'an Jiaotong University, Shaanxi 710049, P.R. China
- ⁵ Xi'an Xiotech Electronics Co, Ltd., Xi'an, Shaanxi 710049, P.R. China

Pyroceram 9606 and Pyrex 7740, and two possible candidate glassy solids, PMMA and BK7, with an absolute low uncertainty of 2%.

Keywords: Bayesian optimization, transient hot-wire, thermal conductivity, solids, finite element method, low uncertainty

1 Introduction

The transient hot-wire technique is a well-established, low-uncertainty absolute technique, with a fully developed theoretical background [1], employed for the measurement of the thermal conductivity of fluids and solids. The evolution of the transient hot-wire technique has been described in details elsewhere [2, 3]. Indeed, if applied properly, with the exception of the critical region and the very low pressure gas region [1], it can achieve uncertainties well below 1 % for gases, liquids, and solids, and below 2 % for nanofluids and melts [3].

There are two transient hot-wire standard test methods for the measurement of thermal conductivity of solids, the American ASTM C1113-99 Resistive Hot-Wire Test Method [4] and the European EN 993-15 Parallel Hot-Wire Test Method [5]. The EN 993–15 is similar to the ISO 8894-2 Parallel Hot–Wire method [6].

- In the case of the resistive mode of the transient hot-wire method [4], the thermal conductivity is obtained from the heat dissipated from a pure platinum wire placed between two solid specimens of the material. The wire acts as both a heat source and as a temperature recorder. The heating wire described in this standard, is usually 0.35 mm - 0.50 mm in diameter, with a length of about 20 cm, resulting in a resistance of about 0.1 Ohm to 0.2 Ohm, which in turn requires high operating power. The large power and the low resistance can easily produce large uncertainties. Moreover, the use of a single wire (instead of two) enhances the errors associated with the end effects of the wire. The thermal conductivity is obtained by using an empirically-selected segment of the temperature rise versus time curve. Contact resistance between the wire and the solid is not accounted for.
- In the parallel mode of the transient hot-wire instrument, instead of the wire acting both as sensor and a thermometer, a thermocouple is placed usually 1.5 cm from the heating platinum wire to register the temperature [5]. However, the errors that exist in the resistive mode of the hot wire, also exist here.

There are very few commercial transient-hot wire instruments today operating according to these standards. For example, the ‘TCT 426 - Thermal Conductivity Tester’ from NETZSCH, operates according to both ISO 8894-2 and ASTM C1113 standards. Although this device can be used to measure the thermal conductivity of solid samples up to $20 \text{ W}\cdot\text{m}^{-1}\cdot\text{K}^{-1}$, there is no quoted uncertainty for the thermal conductivity value and it requires two large samples (250×125×75 mm). Also no information is provided for the material and size of

the hot wire employed. The software used to calculate the thermal conductivity value of the samples designates an empirical evaluation range in the temperature increase curve and hence the uncertainty of the results is increased. Another commercial instrument is the 'THW-S' from Thermtest Inc which uses a 50 mm length and 0.1 mm diameter wire to measure samples (two are required) as small as 1 mm diameter and 50 mm in length. However, the instrument is limited to measuring solid samples with thermal conductivity in the range of 0.01 to 0.2 $\text{W}\cdot\text{m}^{-1}\cdot\text{K}^{-1}$ with an uncertainty of 5 %. Another drawback of this instrument is that its software identifies empirically and removes the non-linear portion or contact resistance at the initial stages of the measurement. This leaves only a linear portion of the temperature increase as a function of time which is then used to determine the thermal conductivity of the samples.

The above instruments are based a lot on empiricism and various calibration procedures, in contrast to the present one that is based entirely on the theory. According to the full theory of the transient hot-wire technique, the thermal conductivity of the medium is determined by observing the rate at which the temperature of a very thin metallic wire increases through time after a step change in voltage has been applied to it, thus creating in the medium a line source of essentially uniform heat flux per unit length that is constant in time. The electric current has the effect of producing a temperature field throughout the medium that increases with time. The thermal conductivity is obtained from the time evolution of the temperature of the wire. We note that the wire acts in a double role: one of a line source of constant heat flux per unit length, and one of a temperature resistance thermometer - provided its material is pure, usually platinum or tantalum. Furthermore, nowadays, to avoid end effects, two wires identical except for their length, are employed. Thus, if arrangements are made to measure the difference of the resistance of the two wires as a function of time, the measurement corresponds to the resistance change of a finite section of an infinite wire (as the end effects being very similar, are subtracted), from which the temperature rise can be determined. It should be mentioned that the temperature rise employed is approximately 3 to 4° K and therefore effects from radiation are negligible.

Since 2002, in a series of papers, the group of Assael [3, 7-16] have described the application of the transient hot-wire technique to the measurement of the thermal conductivity of solids. In the particular case of solids, to overcome the difficulties arising from the air gap between the wires and the solid samples, the experimental setup is different. The two wires are placed inside a soft silicone layer which is squeezed between two samples of the solid whose thermal conductivity is to be measured. This way air gaps are avoided and the contact is excellent. A full theoretical model was developed, with equations solved by a finite-element method (FEM) applied to the exact geometry, and thus allowing an accurate, absolute determination of the thermal conductivity of the solid [8, 11]. By obtaining the temperature rise from the wire's resistance measurement, at very short times the properties of the soft silicone layer are first obtained, and

consequently, at longer times the properties of the solid. The absolute uncertainty achieved in this way is about 1 %, and the technique is only hindered in temperature by the melting temperature of the soft silicone layer.

However, the implementation of the aforementioned methodology showed the following hurdles:

- The preparation and handling of the transient hot-wire sensor is quite difficult and requires the participation of a well-trained user.
- The sensor cannot be easily transferred since it lacks robustness.
- The required post-processing of the experimental data for the calculation of the thermal conductivity of a solid sample requires a trial and error procedure which, even for an expert user, may require up to 10 h.
- The electronic circuit required to perform the measurements (Wheatstone-type bridge, accurate digital power supply and voltmeter) is large in size, and thus, any thoughts of portability are prohibited.
- The FEM software used for the calculation of the thermal conductivity was the commercial COMSOL Multiphysics suite, which is not the ideal tool for this problem.

In this paper a novel implementation of the transient hot-wire technique for the measurement of the thermal conductivity of solids is presented. The new instrument overcomes all the previous drawbacks and provides a tool for measuring the thermal conductivity of solids with low absolute uncertainty. More specifically, the new instrument includes a novel transient hot-wire sensor design with platinum wires, a newly designed compact portable printed electronic board, and a novel Finite Elements Method software suite, which employs Bayesian Optimization, in order to automate the procedure. Bayesian Optimization is a state-of-the-art sequential design strategy for global optimization of black-box functions from the field of Machine Learning. Our revolutionizing proposed methodology exhibits radical speedups of up to 120×, compared to previous approaches. The key of its efficiency lies in the multiple optimization steps applied, that considerably reduce the simulation time, and the number of simulations performed; achieving convergence only in a few minutes.

2 Experimental

2.1 The hot-wire sensor

As already mentioned, the transient hot-wire method is based on the observation of the temporal temperature rise of a thin vertical wire immersed (or embedded) in the test material. The wire is initially at equilibrium and a step voltage is applied to it. In this way, electrical current flows through the wire and heats it up. The wire acts both as a line heat source of uniform constant heat flux per unit length, producing a time dependent temperature field inside the test material, and

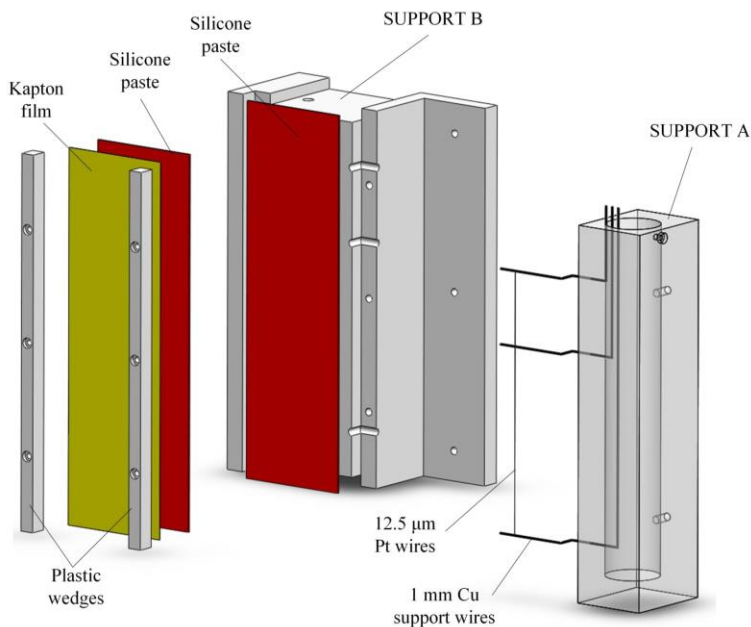


Fig. 1 The new sensor design

as a thermometer registering the temporal resistance change and thus its temperature. Based on the pioneering idea of Harman [17], two identical wires differing only in length are employed in order to compensate for the end effects of the wires [18]. The evolution of the wire's temperature depends on the thermal conductivity of the test material. Thus, the thermal conductivity of the test material can be calculated by monitoring the temperature rise of the wire taking into account the properties of the wire and the surrounding material, as well as the geometry of the wire's enclosure.

In the case of measuring the thermal conductivity of solids the main problem confronted is always the existence of contact resistance between the wires and the solid sample. The contact resistance is a temperature discontinuity that inevitably appears in every contact between two solid materials with quite different thermal properties, when a heat wave is transferred from one solid to the other. In order to render negligible the effects of the contact resistance, the wire is embedded in a flat layer of soft silicone paste [8, 13]. Heat is transferred from the wire to the solid via the silicone paste.

The new sensor is shown in Fig. 1. The sensor is composed of two 12.5- μm -diameter platinum (Pt) wires of 5 and 2 cm length placed one after the other. These lengths are the minimum possible to ensure that after subtracting the end effects, we still have a finite section of an infinite wire. The wires are spot-

welded on 1 mm diameter copper (Cu) support wires that are flattened to 0.6 mm at their ends. The Pt wires are embedded in the center of an exactly 1.2 mm thick soft silicone-paste layer that rests on the one side on a plastic support. On its other side, the solid sample to be measured is placed.

The sensor assembly is performed in the following two steps:

- a) The three 1-mm-diameter copper wires are placed in 3 holes in plastic Support A. They take their final shape, and the three holes in the plastic are sealed with epoxy glue. On the one side of the three copper wires an electric connector is soldered and pushed on top of Support A (see Fig. 1). The other side of the copper wires is flattened to 0.6 mm at their ends and the two 12.5- μm -diameter platinum (Pt) wires of 2 and 5 cm length are spot welded one after the other. Support A is now ready for measuring the thermal conductivity of a fluid by simply immersing it in the fluid. This is one of the main advantages of this sensor, as before being applied to solids, the proper use of the wires, electronic systems, and the software can be checked by measuring the thermal conductivity of a known liquid (see Section 3.1).
- b) In a specially made base, one 25- μm -thick polyimide film (Kapton, Dupont), 10 \times 6 cm is held, while soft silicone paste (Polymax, Bison) is laid over it. A second thin film of silicone paste is also laid over the plastic Support B. Consequently, Support A with the 2 wires, is placed on top of Support B and screwed tight. Finally, the Kapton film with the silicone layer is placed over all of them. Next step is to squeeze the sensor tight, in a specially made base, in order to end up with a soft silicone layer of 1.2 mm thickness exactly. The soft silicone paste, requires around a week to dry, but it still retains some elasticity. After that period the sensor is taken out of the base, and two plastic wedges are used to secure the sensor and the Kapton film.

Hence, the resulting sensor is composed of the plastic material over which there is the 1.2-mm-thick soft silicone layer, with the wires embedded inside. A polyimide film protects the soft silicon layer on its other side. This assembly ensures that the Kapton film protects the silicone paste and that the wires are located in the middle of the silicone layer.

To measure the thermal conductivity of a solid sample, the sensor is placed on top of the sample and an extra 1 kg metallic weight is placed over the sensor in order to provide a gentle pressure to the surfaces (Fig. 2). In the above setup the heat is transmitted from the wire, through the silicone paste, to the solid sample on the one side and the plastic support on the other side. We do note that in our previous design, the sensor was composed only of a 1.2-mm-thick silicone layer protected by Kapton on both sides and with the wires embedded in it. This arrangement was squeezed between two blocks of the same sample material making the wires with the silicon paste layer very fragile.

- The main ameliorations achieved in the new sensor design are:
- the use of the soft silicone layer renders negligible the effects of the contact resistances between the wires and the sample,
 - the new design provides robustness and portability to the sensor, and ensures that the thickness of the silicone paste is known accurately.

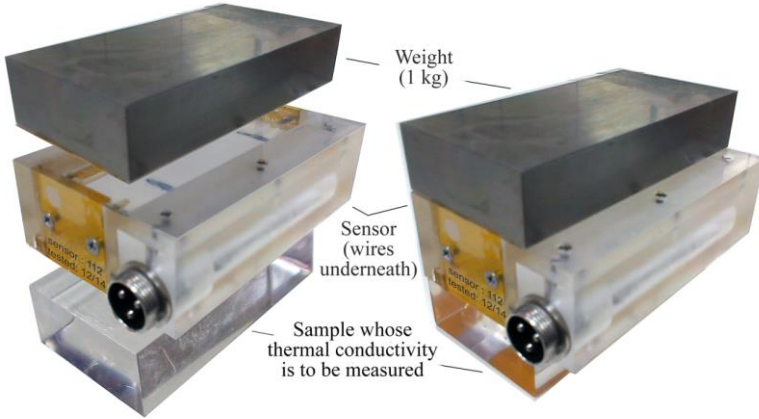


Fig. 2 Sensor assembly with sample and weight

2.2 Working equations

The working equations for the new sensor are similar to those used in the previous designs [8, 13]. For each layer-material, the appropriate partial differential equation for heat transfer needs to be solved. The problem is solved in two dimensions (as the wire is considered infinite in the z -direction i.e. its axis), where the x -axis is parallel to the silicone paste and the y -axis is perpendicular to it. Thus, if λ ($\text{W}\cdot\text{m}^{-1}\cdot\text{K}^{-1}$), denotes the thermal conductivity, T (K), the absolute temperature, t (s), the time, ρ ($\text{kg}\cdot\text{m}^{-3}$), the density, c_p ($\text{J}\cdot\text{kg}^{-1}\cdot\text{K}^{-1}$), the heat capacity at constant pressure, r_0 (m), the wire diameter, and $a = \lambda / (\rho c_p)$ ($\text{m}^2\cdot\text{s}^{-1}$), is the constant thermal diffusivity, the working equations are [13]:

- For the platinum *wire* and $t \geq 0$ and $0 \leq r \leq r_0$,

$$\rho_w c_{pw} \frac{\partial T_w}{\partial t} = \lambda_w \left[\frac{\partial^2 T_w}{\partial x^2} + \frac{\partial^2 T_w}{\partial y^2} \right] + \frac{q}{\pi r_0^2}. \quad (1)$$

b) For the *silicone* paste (and the protective polyimide),

$$\rho_m c_{pm} \frac{\partial T_m}{\partial t} = \lambda_m \left[\frac{\partial^2 T_m}{\partial x^2} + \frac{\partial^2 T_m}{\partial y^2} \right]. \quad (2)$$

c) For the *sample* to be measured and the *plastic support*,

$$\rho_s c_{ps} \frac{\partial T_s}{\partial t} = \lambda_s \left[\frac{\partial^2 T_s}{\partial x^2} + \frac{\partial^2 T_s}{\partial y^2} \right] \quad (3)$$

It shall be noted that Eq. (3) is applied on top to the plastic support, and underneath to the solid sample material. Also the protective polyimide film (25 μm thick) is in essence incorporated as part of the silicone paste properties since its properties are very close to the silicone paste properties and it has negligible effect on the temperature response of the wire.

The above equations, subjected to initial and boundary conditions, are solved numerically using the finite element method (FEM) for the exact geometry of the sensor, and the temperature rise calculated by FEM is compared with the experimental one. Before proceeding with the description of the innovative FEM model, the electronic bridge used to obtain the experimental temperature rise will be described.

2.3 The Electronic Bridge

The purpose of employing an electronic bridge in the transient hot-wire instrument is twofold: first, to measure the evolution of the resistance change of a finite segment of infinite wire (by automatically compensating for axial heat conduction from the wire ends), and second, to ensure that a known constant heat flux is generated in the hot wires [13].

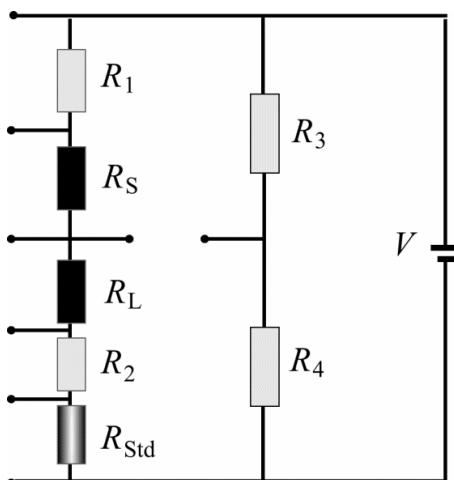
The first investigator to use a bridge that fulfils the above requirements was Haarman in 1971 [17]. He used a Wheatstone bridge to measure the resistance difference between two identical wires with different length. In that way, the end effects of the wires were compensated. Since then, and following the advances in electronics and computers, the electronic bridges employed together with transient hot-wire instruments have tremendously been developed.

To achieve a series of equilibrium states in the Wheatstone bridge, with a wire in each opposite arm, various configurations have been employed. In the 1970's, following the initiation of the heating of the wires, the resistors in the one arm were automatically changed six times, to obtain six new equilibrium positions and thus six resistance values of the wires [19-22]. In order to increase the number of resistance measurements at one experimental run, an alternative design was employed in the 1980's and 1990's [23, 24]. In this design instead of

changing the resistances of the upper right arm, the voltage of the lower right arm was changed to predetermined, by a computer, values. This electronic setup was able to register up to 32 equilibrium points for a run up to 1 s.

In order to attain many more resistance measurements a new design was employed after 2000 [8, 13]. The fundamental principle of this computer controlled Wheatstone-type bridge is the same as previous designs, with the difference that upon initiation of the current through the wires (R_S and R_L), all voltages in the bridge are recorded, see Fig. 3. The wires' resistances over time are calculated from the voltage ratios and a known standard resistance R_{Std} placed on the same bridge's arm with the long wire. This way, during a transient run a large number of experimental data points (usually 500-1000 points) are recorded.

Fig. 3. Typical automatic bridge designs



The electronic bridge developed for the new instrument employs an FPGA architecture CPU to control the output voltage and data processing while it has all the characteristics of the previous one. The circuit design (shown in Fig. 4) includes a known standard resistance R_{Std} (10 Ohm), the resistances R_1, R_2, R_3 and R_4 of the Wheatstone-type bridge, a 220V AC power supply unit, a control FPGA (Field Programmable Gate Array) chip EP2C8Q208, a high precision analogue-to-digital (A/D) converter (LTC2440) and a USB 2.0 chip. The board has five data acquisition channels (see Fig. 4), and thus in order to synchronize the data acquisition process through the A/D converter, the FPGA chip is programmed using Verilog hardware description language (Verilog HDL) and System on a Programmable Chip (SOPC) technology. The board is operated by a portable computer through a USB connection.

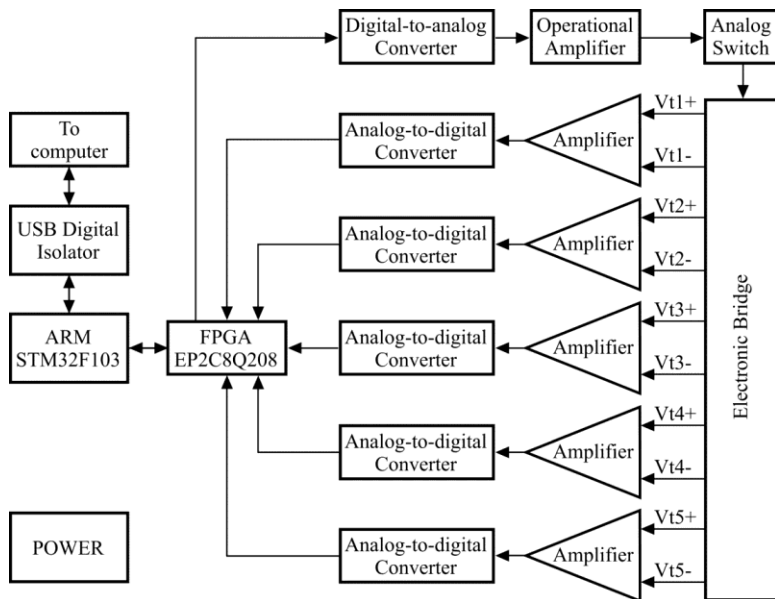


Fig. 4 Circuit diagram

The working equations of the Wheatstone-type bridge are described in detail elsewhere [13]. As mentioned in [13], the procedure to obtain the absolute temporal resistance change upon applying a voltage requires the knowledge of the actual steady state resistance values of the two wires (resistance values at zero voltage, i.e. at room temperature). These values are obtained automatically by the new board by a steady-state measurement before the transient one. Thus, solving the bridge equations [13] the absolute resistance change of the central portion of the long wire is obtained and from that, the actual temperature rise at the surface of the wire.

The principal characteristics of the new electronic circuit are:

- a) It is compact, portable and easy to connect to a computer. Also, it has a user-friendly interface (Fig. 8).
- b) It has the ability to begin measurements from 1 ms after the initiation of heating and to obtain a large number of data points (usually 500 in one run).
- c) It registers the experimental time through the A/D converter with a resolution of 1 μ s.
- d) All required bridge resistances are mounted on the new board.
- e) Change of the wires' resistances over time is obtained by recording all voltages at the left arm and the off-equilibrium signal of the bridge, at predetermined times.

2.4 FEM analysis software suite

The FEM analysis software suite accompanying the new transient hot-wire sensor, is one of the important novelties of the present work. The heat wave produced by the wire is transferred to the solid through the silicone layer. The heat transfer equations (1) – (3) need to be solved for each layer separately, but as mentioned before, this cannot be done analytically. Instead they are solved numerically using the Finite Element Method (FEM), over the modelled geometry of the sensor.

FEM is a numerical analysis technique applied to a wide variety of problems and scientific fields. The basic idea is that a certain given domain can be represented by a mesh of small, interconnected geometric shapes, the finite elements. This paves the way for detailed discretization and modeling of the different materials and areas of interest. Subsequently, the heat equations are solved over the domain of the modeled mesh, and the goal of our software is to estimate the optimal thermal conductivity of the measured material, where the simulation matches the experimental observations. Hitherto, other applications of the transient hot-wire technique [7-11] make use of the commercially available COMSOL Multiphysics finite-element package, to model and analyze the geometry of the sensor. The procedure to extract the thermal conductivity value of the measured material was based on iterative inverse analysis. The unknown thermal properties were calculated by iterative adjustments of the estimated values until COMSOL Multiphysics calculated temperature rise, was superimposed satisfactory to the experimental one. The intuition behind these iterative adjustments was very similar to ‘binary search’, a fundamental dichotomic divide and conquer search algorithm. The whole process was performed manually by the user and could take up to 10 hours.

To the best of our knowledge, the presented approach is the fastest and most accurate method for estimating thermal conductivity of solids, published in literature. The overall procedure in order to estimate thermal conductivity, can be described in the following steps:

- 1) Sensor geometry and mesh construction
- 2) FEM simulation
- 3) Bayesian Optimization to estimate the thermal conductivity
- 4) Further computational optimizations

2.4.1 Sensor geometry and mesh construction

One of the most fundamental parts in FEM, is the construction of the mesh model based on a given initial geometry. For this task, the exact geometry of the sensor was modeled as 2D Mesh using the open-source Gmsh CAD application [25]. In general, the quality of the mesh is related to the ability of accurately modeling the initial geometry. Therefore, the accuracy of the FEM results is

directly connected, and proportional, to the quality of the modelled mesh where the system of equations is solved. Finally, using tiny sized shapes would increase the mesh quality, but may substantially hinder the computational complexity of the problem solved, and, as a result, the execution time.

The efficient construction of the mesh becomes even more crucial, when the described geometry varies from such tiny scales to large surfaces. In this case, the mesh has to be repeatedly optimized in order to achieve the optimal performance and quality trade-off. The geometry of the present mesh varied from the order of cm size in the support and sample, to micron sizes close to the wire. In order to achieve such equilibrium between performance and quality, the 2D Frontal Triangulation algorithm described by Rebay [26], was utilized. The algorithm drastically increased the performance by doing refinements and grouping areas, while at the same time it retained the quality of the results. Finally, additional manual optimization, in terms of execution time, was performed by adding ‘latent’ points in our geometry to refine the quality of the area of interest around the wire. The resulting mesh from the sensor’s geometry is illustrated in Fig. 5.

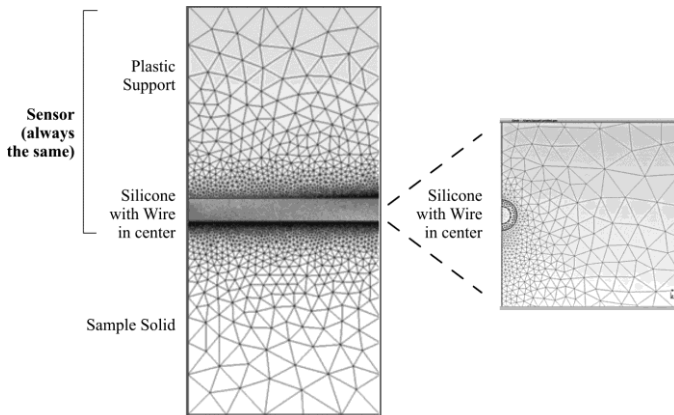


Fig. 5 Mesh details

2.4.2 FEM simulation

Previous applications of the transient hot-wire technique [7-11] made use of the commercially available COMSOL Multiphysics finite-element package to simulate the heat flow, using the iterative inverse analysis. This significantly limits the automation achieved with the present tailor-made software. The present novel FEM analysis suite employs the open-source FiPy Partial differential equations solver framework. FiPy is developed and maintained by NIST (USA) [27], and was used for pre-processing and solving the finite

elements. The framework is written in Python, based on the scientific SciPy and the numerical NumPy tools, while it is characterized by its reliability and flexibility.

Using the mesh in Fig. 5, generated in the previous step, the present FEM analysis suite performs the following two tasks (Fig. 6):

- 1) Given a value of thermal conductivity for the measured material, it solves heat flow using FEM and computes the temporal temperature-rise curve at the predetermined time intervals of the experiment.
- 2) Subsequently, it compares the calculated curve with the experimental one. The procedure is repeated iterating over the possible thermal conductivity values of the solid sample until the two curves coincide, meaning that the simulation matches the experimental observations. Therefore, the selected thermal conductivity correctly expresses the attributes of the sample material.

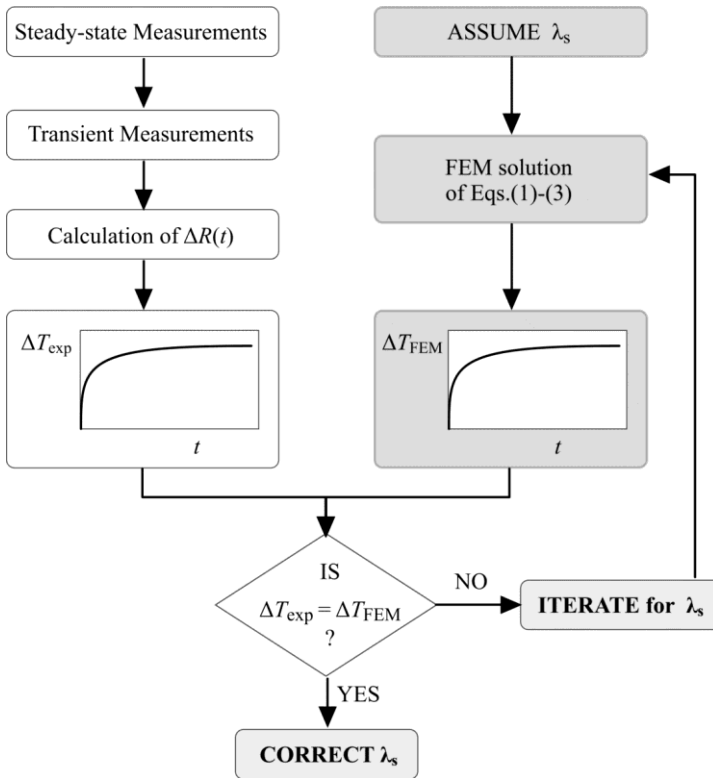


Fig. 6 Procedure to obtain the thermal conductivity value

Hitherto, the methodology followed, would start with an initial value of the thermal conductivity, λ , and the subsequent values were chosen using the binary search algorithm. More specifically, the temperature rise, ΔT values of the two curves would be subtracted and a linear function would be fitted in their differences, in order to compare them. This linear function reflects the degree of similarity between the simulated and the experimental observations. While iterating, if the slope was positive, the right margin of the search space would be redefined with the current λ value and vice versa for a negative slope. The iterations would stop when a threshold close to zero was reached, meaning that the two curves coincide. Although this method is robust, it lacks of efficiency, as it does not take into consideration the steepness of the slope, as well as, previous evaluations of the thermal conductivity. Thus, it requires more exploration in the search space.

2.4.3 Bayesian Optimization to estimate thermal conductivity

The aforementioned procedure, for estimating the thermal conductivity value through FEM simulations, could be automated and formed as an optimization problem, where the objective function to be minimized is expressed as a measure of distance of the experimental temperature rise, ΔT_{exp} and the calculated by FEM temperature rise, ΔT_{FEM} curves. This measure of distance is again defined as the slope of the linear function fitted in the differences of the two curves. Additionally, this time an L2 regularizer was used to penalize the influence of possible noise in the measurements, making the method robust to outliers. However, the problem is hard and common optimization techniques would be ill-suited. The reason is that, the problem cannot be expressed in a simple closed mathematical form, as it incorporates the FEM, and, therefore, its derivatives are unknown. In such cases, the gradients could be approximated numerically by evaluating the function multiple times in small steps and calculating the slope. However, each simulation takes about a minute, making the evaluation of a single new parameter over the unknown function extremely expensive in terms of computational time. Finally, as a plethora of environment factors may have a slight instantaneous impact on an experimental observation, the objective function is considered to have a small ratio noise in the observed values.

In order to overcome these problems, Bayesian optimization, a state-of-the-art method from the field of Artificial Intelligence and Machine Learning, was utilized. Common applications of the method include the optimization of Artificial Neural Networks (Snoek *et al.* [28, 29]), Information Extraction (Wang and de Freitas [30]), as well as, Robotics, Reinforcement Learning (Brochu *et al.* [31]) and Geostatistics (Assael *et al.* [32]). Bayesian optimization has proven to be a popular and successful methodology for global optimization of expensive black-box functions. It is used to find the global minimum of generally non-convex, multi-modal functions whose derivatives are unavailable, and when the

evaluations of the objective function are often only available via noisy observations. Hence, it consists the perfect choice for the aforementioned optimization problem.

In general, according to Bayesian optimization, the goal of global optimization is to find the optimum

$$x^* = \int_{x \in X}^{\arg \max} f(x) \tag{4}$$

of an objective function $f: X \rightarrow \mathbb{R}$ over an index set $X \subset \mathbb{R}^d$, where d is the number of parameters to be optimized. The approach of Bayesian optimization may be understood in the setting of sequential decision making, whereby at the t -th decision iteration, we select an input $x_t \in X$ and observe the value of the black-box reward function $f(x_t)$. The returned value y_t may be deterministic, $y_t = f(x_t)$, or stochastic as in our case, $y_t = f(x_t) + \varepsilon_t$, where ε_t is a noise process.

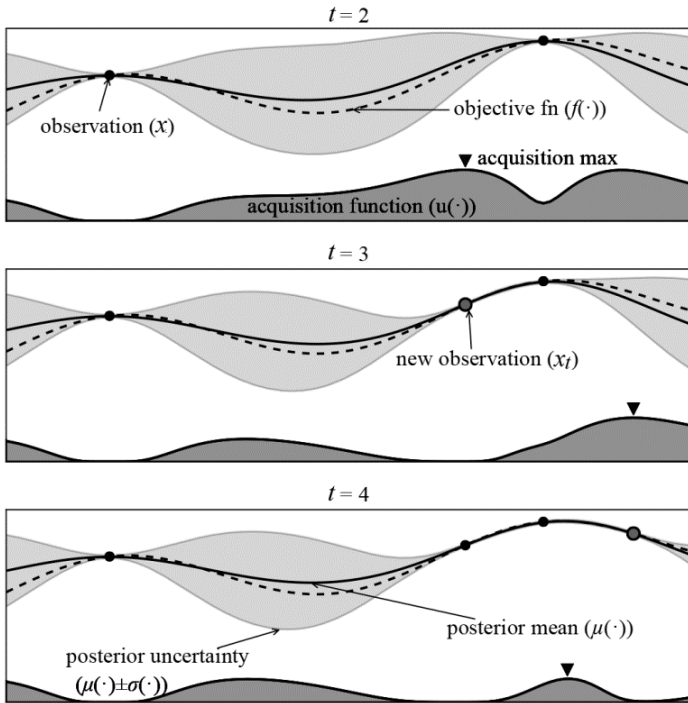


Fig. 7 Three Bayesian Optimization iterations on a 1D black-box toy maximization problem. The black line represents the GP estimated mean function, while the dashed line depicts the real black-box objective function. The light gray areas show the credible intervals of the GP, and the dark gray line represents the value of the acquisition function, that will be used to select the next candidate value to query our objective function. Finally, the dots represent the observations so far [31].

Since the function is unknown, we use a Bayesian prior model to encode our beliefs about its smoothness, and an observation model to describe the data $D_t = (\mathbf{x}_t, \mathbf{y}_t)_{i \leq t}$ up to the t -th iteration. Assuming that close input values will have close outputs, we use Gaussian processes (GP) which popular priors for Bayesian optimization, as they offer a simple and flexible model to capture the behavior of the function. Using these two models and the rules of probability, we derive a posterior distribution $p(f | D_t)$ that can in turn be used to build an acquisition function u , to decide the next input query \mathbf{x}_{t+1} . The acquisition function trades-off exploitation and exploration in the search process. In our implementation we used the Expected Improvement acquisition function, which is considered one of the most popular and robust choices. For a comprehensive introduction of Bayesian optimization we refer the reader to Brochu *et al.*[31], and Snoek *et al.*[28], while an example run on a 1D maximization problem is illustrated in Fig. 7.

Bayesian Optimization substantially reduced the execution time as, at each iteration the algorithm tried to explore and exploit the search space in the most efficient way, taking into consideration all the previous output values. Thus, it significantly outperformed the previously used binary search. More specifically, binary search would take about 10-12 iterations in the search space of $\lambda \in [0.1, 4] \text{ W}\cdot\text{m}^{-1}\cdot\text{K}^{-1}$, while Bayesian optimization would require only 5-6 iterations. Given that each simulation takes about a minute this is a substantial 2x speedup in the overall execution time.

2.4.4 Further computational optimizations

After reducing the number of iterations, the next step was to reduce the simulation time of each iteration. To achieve that, two more optimization steps were applied in our FEM analysis software:

- 1) The first optimization step reduced the number of evaluated time steps. More specifically, an experimental run usually consists of 500 ΔT_{exp} values (1 value every 0.02 s). Our empirical evaluation showed that 280 exponentially growing time steps is a reliable sample, that still allows us to compare the curves without any loss in accuracy.
- 2) The second optimization step made use of previously calculated values for the first time steps, significantly reducing the number of new time-steps. Our experiments on modelling the sensor geometry, showed that until 0.1 s the heat has not reached the measured material. Hence, the calculated states of all the mesh cells until that point can be saved and reused in every new simulation.

2.4.5 Software Suite

The novel FEM software suite that incorporates all the aforementioned optimizations was validated against COMSOL Multiphysics. Using the same sensor geometry and the same experimental data, both tools resulted the same

thermal conductivity values for each of the test samples. Furthermore, the present software suite has a user-friendly interface, specially designed for the needs of this process, that is depicted in Fig. 8.

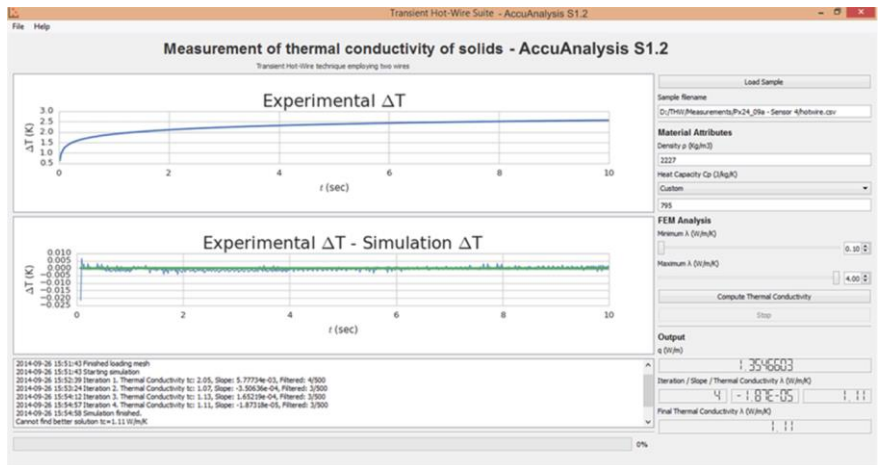


Fig. 8 FEM software user interface showing a typical experimental temperature rise as a function of time for Pyrex 7740 at 298 K

The hardware used to perform the simulations includes an Intel® Core™ i5-4200M Processor (2.50 GHz up to 3.10 GHz, 3M Cache) with 4 GB RAM. The results show, that using the present novel method and all the optimizations mentioned above, the function converges to the optimum in about 5-6 iterations, and less than 5 min. This is a radical 120x speedup, compared to the previous procedures described in literature, which could take up to 10 hours.

The major contributions and novelties of our FEM analysis suite are the following:

- a) For the first time, to our knowledge, the whole iteration process was fully automated.
- b) The simulations use FEM offering low absolute uncertainty of 2%.
- c) Using the Bayesian Optimization method and the additional optimization steps, our approach is automated and outputs the correct thermal conductivity of the sample material within 5 minutes. This offers a 120x speedup, and compared to previous approaches it revolutionizes the speed, as well as the accuracy, of measuring the thermal conductivity of a solid.

3 Results and Discussion

3.1 Validation of the technique

One of the greatest advantages of the new experimental setup is that the performance of the instrument can be tested by measuring the thermal conductivity of a reference liquid. More specifically, before placing the 2 wires fixed in the Support A, in the soft silicone paste layer, they are inserted in toluene and its thermal conductivity is measured. In this case, the same FEM model is used but as it is a single medium all properties of the other three layers (silicone, solid support, sample solid) are set equal. Hence, the thermal conductivity of toluene can easily be measured. Toluene has been proposed by the Subcommittee on Transport Properties of the International Union of Pure and Applied Chemistry as a standard reference thermal-conductivity liquid with an uncertainty of 0.6 % [33]. The experimental thermal conductivity value obtained using the FEM software is always within this uncertainty. Consequently this comparison, allows us to check the excellent operation of a) all electronic components and bridge operation, b) our measuring procedure, c) the resistance change measurements, d) the temperature rise calculation, and e) the FEM thermal conductivity (for single fluid) calculations.

In Fig. 9 a comparison between two runs, one from the new FEM tool, and one from COMSOL Multiphysics employed till now, is shown. In both runs the input parameters to the model correspond to those of a measurement in liquid toluene. As the thermal conductivity is obtained from the slope of the line, the agreement between the values obtained from the two software is excellent, and furthermore both values of the thermal conductivity obtained agree with the proposed value [33], to better than 0.5%.

Fig. 9 Comparison between the temperature rise calculated by the new FEM software (- -), and the temperature rise calculated by COMSOL Multiphysics (—), as a function of time for toluene at 298 K

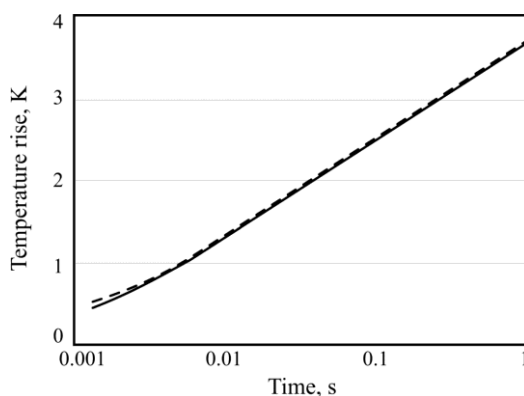


Figure 10 shows a typical experimental temperature rise as a function of the time, during a measurement of a solid sample. To obtain the 4° K temperature rise, the voltage applied was about 5 V and the resulting current in the wires, was about 80 mA. The temperature rise was kept as low as possible to avoid radiation effects, while at the same time still achieve the required precision. This criterion determines the required current and voltage. In the same figure the calculated temperature rise from the new FEM software is also shown. Full agreement is observed over a time range of five orders of magnitude as the heat pulse transmits through four different materials (wire, silicone paste, plastic support, sample solid). The first part of the curve is related to the properties of the platinum wire, the second part corresponds to the silicone paste and the last part to the properties of the solid. Thus, running the experiment:

- at very low times (heat wave still in silicone), the properties, $(\rho_m c_{pm})$ and λ_m , of the silicone paste can be obtained.
- Then by replacing the sample solid, with another piece of the plastic support, we eliminate all the unknown parameters apart from the properties of the plastic support, $(\rho_s c_{ps})$ and λ_s , since the properties of silicone have already been obtained. Thus, these properties can also be estimated

Therefore the **only unknown variable** remaining to be obtained during a run, is the thermal conductivity of the sample solid (since (ρc_p) are known). It should be noted that since the full heat equations are solved, the thermal diffusivity could also be obtained. In that case, the product (ρc_p) would need to be obtained by the algorithm. This requires an extra iteration, which will result to additional quite large computational time. Since at present we are only interested in measuring very accurately the thermal conductivity (and keeping in mind that there are better ways to measure more accurately the heat capacity), the challenge of the diffusivity will be dealt in the near future.

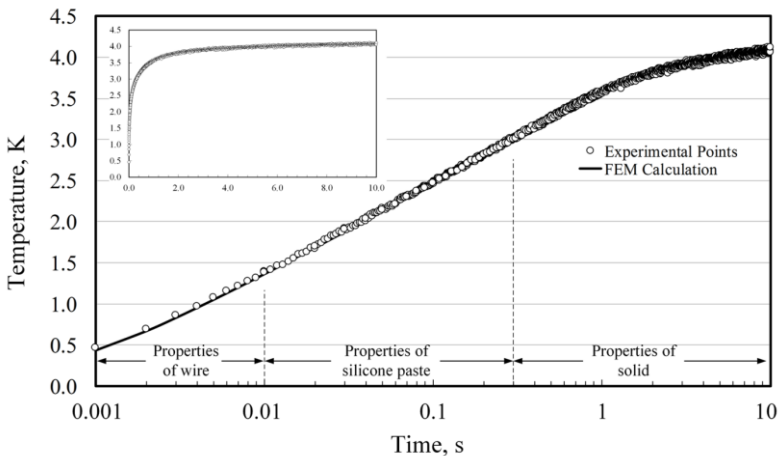


Fig. 10 Typical temperature rise as a function of time of BK7 at 298 K

3.2 Uncertainty analysis

As already mentioned, the technique employed is an absolute technique. The final uncertainty of the method consists of two separated parts: firstly the uncertainty arising from the experimental procedure and the electronic configuration used, and secondly the uncertainty due to the use of the finite element method.

As far as the uncertainty of the experimental setup is concerned, it is associated with the uncertainty of the variables that affect the wires' resistances and the experimental time measurement. More specifically the related variables are:

a) Supply voltage

The voltage applied to the bridge, and its evolution during a transient experimental run, is monitored digitally with an uncertainty of about $\pm 1 \mu\text{V}$. The recorded voltage differences are transformed into resistances changes and consequently on temperature differences of a wire with no ends. The effect of this parameter on the temperature rise of the wire is estimated to be of the order of $10^{-4} \%$.

b) Experimental time

The experimental time is measured and registered through the electronic board with an uncertainty of $1 \mu\text{s}$. In the calculation of thermal conductivity value, the logarithm of time is used and therefore its influence on the uncertainty of the obtained value is lower than $10^{-3} \%$.

c) Temperature coefficients of resistance

This was obtained by employing a Class I platinum resistance thermometer, with an uncertainty of $\pm 1 \text{ mK}$, which has no measurable effect in the temperature rise of the wire.

d) Sensor thickness

The experimental sensor is constructed so that the thickness of the silicone paste film is defined and equal exactly to 1.2 mm . Thus, it does not affect the uncertainty of the technique.

According to the Joint Committee for Guides in Metrology [34], the combined uncertainty $u_c(y)$ of the quantity $Y(x)$, is the positive square root of the combined variance $u_C^2(y)$ obtained from:

$$u_C^2(y) = \sum_{i=1}^N \left(\frac{\partial Y(x)}{\partial x_i} \right)^2 u^2(x_i), \quad (4)$$

where $u^2(x_i)$ are the variances of the input quantity x_i . The partial derivatives of $Y(x)$ are called sensitivity coefficients and describe how the output estimate y varies with change in the values of the input estimates x_1, x_2, \dots, x_N . Applying Eq.(4) in the aforementioned variables, the estimated **uncertainty of the experimental setup** is no more than **0.1%**.

Uncertainty due to the use of the finite element method is obtained through a sensitivity analysis which evaluates the effects that the design parameters of the FEM model have on the calculated temperature rise and therefore on the calculated thermal conductivity value. In order to perform the sensitivity analysis a typical solution of the FEM model was considered, and consequently the design parameters of the model (geometrical or material properties) were altered and the effect on the calculated thermal conductivity value of the solid sample was recorded. The design parameters analysed are:

- Wire diameter
- Heat flux from the wire
- The thermal conductivity and the product (density \times specific heat capacity) of the silicone paste
- Support B thermal conductivity and the product (density \times specific heat capacity)
- Solid sample thermal conductivity and the product (density \times specific heat capacity)

Applying Eq.(4) for the above parameters, the estimated **uncertainty of the Finite Element Method applied** is no more than **1.5%**.

3.3 Measurements

The new transient hot-wire instrument was employed for the measurement of the thermal conductivity of solids at room temperature (298 K). The materials studied are two thermal-conductivity reference materials, Pyroceram 9606 (designated as glass ceramic BCR-724), Pyrex 7740 (designated as BCR-039), and two possible thermal-conductivity reference candidate glassy solids, Polymethyl Methacrylate (PMMA) and Borosilicate Crown Glass (BK7). The above four material were selected in order to use the new hot-wire instrument, for measuring the thermal conductivity of solids over a range of 0.2 to 4 W \cdot m⁻¹·K⁻¹. The minimum dimensions of a sample should be: a) length about 10 cm (as the total length of Pt wires is 7 cm), b) width more than 2 cm (to cover a large part of the sensor), and c) thickness larger than 0.5 cm (to avoid heat losses on the other side of the sample).

Pyroceram 9606 is an opaque glassy ceramic, originally developed by NASA, and since it is particularly well defined and thermally stable, it was proposed as a standard reference material for thermal conductivity by the National Institute of Standards and Technology (NIST), U.S.A [35]. Moreover, since May 2007, Pyroceram 9606 is supplied by the European Commission Institute for Reference Materials and Measurements (<http://www.irmm.jrc.be/>) as a certified thermal-conductivity and thermal-diffusivity reference material (designated as glass ceramic BCR-724) up to 1025 K [36]. This certification was the outcome of a research project, funded by the European Union under the

'Competitive and Sustainable Growth' program ("HTCRM - High Temperature Certified Reference Materials," Contract SMT4-CT98-2211/2003). The uncertainty of the certified thermal conductivity value was $\pm 6.5\%$, while that of the thermal diffusivity was $\pm 6.1\%$. The specimens of Pyroceram 9606 employed in the present work were made by Corning Inc., New York and purchased from Anter Corporation (now TA Instruments), Pittsburgh, PA, U.S.A. The samples have dimensions of $5 \times 10 \times 2 \text{ cm}^3$ and their density was found by weighing them and determining their volume equal to $2,596 \text{ kg} \cdot \text{m}^{-3}$ at 298 K.

Pyrex 7740 is a well-known Type I, Class A borosilicate glass, which conforms to ASTM E438 [37], and since 1990 it is considered as a certified reference material for thermal conductivity, BCR 039, by the European Union of Reference Materials and Measurements [38]. The use of Pyrex 7740 as a reference material has its roots back to the mid-1960s, when Powell *et al.* published recommended thermal conductivity values [35]. Pyrex 7740 has a low coefficient of expansion, which allows to be manufactured in relative heavy walls giving it mechanical strength, while retaining reasonable heat resistance. Moreover, it is highly resistant to chemical compounds such as strong acids, alkalis, *e.t.c.*, and can withstand temperatures up to 760 K. Therefore, due to its excellent thermal and mechanical properties, Pyrex 7740 is used in many laboratory and industrial applications. The samples of Pyrex 7740 employed in the present work were supplied by Anter Corporation (now TA Instruments), Pittsburgh, PA, U.S.A. The samples have dimensions of $5 \times 10 \times 2 \text{ cm}^3$ and their density was found by weighing them and determining their volume equal to $2,227 \text{ kg} \cdot \text{m}^{-3}$ at 298 K.

PMMA or Perspex is an amorphous, colorless thermoplastic material of excellent optical transparency and a luminous transmittance of about 92%. It has good abrasion resistance and dimensional stability but is brittle and notch sensitive. Its water absorptivity is very low in comparison with other polymer materials. PMMA was proposed by the National Physical Laboratory (NPL), U.K, as a possible candidate for thermal conductivity reference standard in 2001 [39]. However a more recent intercomparison between 17 laboratories organized by Physikalisch-Technische Bundesanstalt (PTB), Germany, showed uncertainties in the thermal conductivity values between 8% to 13%, which far exceeded the laboratories quoted uncertainties. Hence, the employment of PMMA as an acceptable thermal conductivity standard is still under consideration. The samples of PMMA employed in the present work were produced by casting and supplied by Degussa Rohm Plexiglas GmbH and were made available by PTB. The samples have dimensions of $5 \times 10 \times 2 \text{ cm}^3$ and their density was found by weighing them and determining their volume equal to $1,200 \text{ kg} \cdot \text{m}^{-3}$ at 298 K.

BK7 is a Borosilicate Crown Glass that is commonly used material for optical components and can be manufactured with outstanding homogeneity. It has isotropic thermophysical properties with an excellent long-term stability. In 2002, an intercomparison between 11 European laboratories was organized by Physikalisch-Technische Bundesanstalt (PTB) aiming to qualify it as a possible

candidate reference material for thermal conductivity in the temperature range 173 K to 773 K [40]. The samples of BK7 employed in the present work were manufactured and supplied by Schott AG, and were made available by PTB. The samples have dimensions of $5 \times 10 \times 2 \text{ cm}^3$ and their density was found by weighing them equal to $2,504 \text{ kg} \cdot \text{m}^{-3}$ at 298 K.

The thermal conductivity of the four solid samples was measured at 298 K with the new transient hot-wire instrument with an uncertainty of 2% and the resulting values are shown in Table 1. In the same table, our previously measured values with another 2-tantalum-wires transient hot-wire instrument developed in the Laboratory [8, 11] are also shown. It is apparent that the present set of thermal-conductivity values agree well with the previous sets of measurements for all four samples and the maximum deviation is -1.77% which is in between the mutual uncertainties of the two instruments.

Table 1 Measured properties of solid samples at 298 K

Solid sample	$\lambda_s (\text{W} \cdot \text{m}^{-1} \cdot \text{K}^{-1})$	$\lambda_{\text{ref}} (\text{W} \cdot \text{m}^{-1} \cdot \text{K}^{-1})$	$\Delta\lambda^a (\%)$	Reference
Pyroceram 9606	3.80	3.83	-0.78	[8]
Pyrex 7740	1.11	1.13	-1.77	[11]
PMMA	0.190	0.189	0.53	[11]
BK7	1.07	1.06	0.94	[11]

$$^a \Delta\lambda = 100 \times (\lambda_s - \lambda_{\text{ref}}) / \lambda_{\text{ref}}$$

4 Conclusion

The paper presents a novel portable instrument suitable for the measurement of the thermal conductivity of solids over a range of 0.2 to $4 \text{ W} \cdot \text{m}^{-1} \cdot \text{K}^{-1}$, with an absolute uncertainty of 2%. The technique employed is the 2-wire transient hot-wire technique, combined with a newly developed finite element software and model, and a new electronic circuit employing an FPGA architecture CPU to control the output voltage and data processing. The novel FEM suite accompanying the sensor, takes advantage of the state-of-the-art Bayesian Optimization method from the field of Machine Learning, as well as, a series of tailor-made problem specific computational optimizations. The combination of both revolutionizes, and radically reduces, the time to obtain the thermal conductivity of a solid to less than 5 minutes. The instrument was successfully used to measure at room temperature the thermal conductivity of two thermal conductivity reference materials, Pyroceram 9606 and Pyrex 7740, and of two possible candidate glassy solids, PMMA and BK7.

Acknowledgements The Laboratory of Thermophysical Properties & Environmental Processes and Tessera Multimedia, gratefully acknowledge financial support under the Operational Program “Competitiveness and Entrepreneurship” (EPAN II), Action: Greece - China Bilateral R&TD Cooperation 2012-2014 (Project number 12CHN68). The authors would also like to thank Dr. Vassili Efopoulos and Ms. Konstantina Marini, from Tessera Multimedia for their help in the administration of the whole project, and Mr G. Matziaroglou for his participation in the test runs.

References

1. M.J. Assael, C.A. Nieto de Castro, H.M. Roder, W.A. Wakeham, Transient methods for thermal conductivity, in *Experimental Thermodynamics, vol. III: Measurement of the Transport Properties of Fluids*, ed. by A. Nagashima, G.V. Sengers, W.A. Wakeham (Blackwell Scientific Publications, 1991), pp. 161–195
2. J.T. Wu, M.J. Assael, K.D. Antoniadis, S.I. *History of the Transient Hot Wire*, in *Experimental Thermodynamics Volume IX: Advances in Transport Properties of Fluids*, ed. by M.J. Assael, A.R.H. Goodwin, V. Vesovic, W.A. Wakeham (RSC Press., London, U.K., 2014), p. 132-138
3. M.J. Assael, K.D. Antoniadis, W.A. Wakeham, *Int. J. Thermophys.* **31**, 1051 (2010)
4. Standard Test Method for Thermal Conductivity of Refractories by Hot Wire (Platinum Resistance Thermometer Technique), ASTM Designation C1113-99 (American Society for Testing and Materials, Philadelphia, U.S.A., 1999)
5. Methods for Testing Dense Shaped Refractory Products - Determination of Thermal Conductivity by the Hot-Wire (Parallel) Method, EN 993-15. (European Committee for Standardization, 1998)
6. Refractory Materials. Determination of Thermal Conductivity. Part 2: Hot-wire methods (parallel), ISO 8894-2 (International Organization for Standardization, Geneva, Switzerland, 2007)
7. K.D. Antoniadis, M.J. Assael, C.A. Tsiglifisi, S.K. Mylona, *Int. J. Thermophys.* **33**, 2274 (2012)
8. M.J. Assael, K.D. Antoniadis, K.E. Kakosimos, I.N. Metaxa, *Int. J. Thermophys.* **29**, 445 (2008)
9. M.J. Assael, K.D. Antoniadis, I.N. Metaxa, D. Tzetzis, *J. Chem. Eng. Data* **54**, 2365 (2009)
10. M.J. Assael, K.D. Antoniadis, D. Tzetzis, *Comp. Sci. Techn.* **68**, 3178 (2008)
11. M.J. Assael, K.D. Antoniadis, J. Wu, *Int. J. Thermophys.* **29**, 1257 (2008)
12. M.J. Assael, S. Botsios, K. Gialou, I.N. Metaxa, *Int. J. Thermophys.* **26**, 1595 (2005)
13. M.J. Assael, M. Dix, K. Gialou, L. Vozar, W.A. Wakeham, *Int. J. Thermophys.* **23**, 615 (2002)
14. M.J. Assael, K. Gialou, *Int. J. Thermophys.* **24**, 1145 (2003)
15. M.J. Assael, K. Gialou, *Int. J. Thermophys.* **24**, 667 (2003)
16. M.J. Assael, K. Gialou, K. Kakosimos, I. Metaxa, *Int J Thermophys* **25**, 397 (2004)

17. J.W. Haarman, *Physica* **52**, 605 (1971)
18. J. Kestin, W.A. Wakeham, *Physica* **92A**, 102 (1978)
19. J.J. De Groot, J. Kestin, H. Sookiazian, *Physica* **75**, 454 (1974)
20. C.A. Nieto De Castro, J.C.G. Calado, W.A. Wakeham, M. Dix, *J. Phys. B: Atom. Mol. Phys.* **9**, 1073 (1976)
21. J. Kestin, R. Paul, A.A. Clifford, W.A. Wakeham, *Physica A: Stat. Mech. Appl.* **100**, 349 (1980)
22. M.J. Assael, M. Dix, A. Lucas, W.A. Wakeham, *J. Chem. Soc., Faraday Trans. 1: Phys. Chem. Cond. Phases* **77**, 439 (1981)
23. G.C. Maitland, M. Mustafa, M. Ross, R.D. Trengove, W.A. Wakeham, M. Zalaf, *Int. J. Thermophys.* **7**, 245 (1986)
24. M.J. Assael, E. Charitidou, G.P. Georgiadis, W.A. Wakeham, *Ber Bunsenges Phys Chem* **92**, 627 (1988)
25. C. Geuzaine, J.-F. Remacle, *Int. J. Num. Meth. Engin.* **79**, 1309 (2009)
26. S. Rebay, *J. Comp. Phys.* **106**, 125 (1993)
27. J.E. Guyer, D. Wheeler, J.A. Warren, *Comput Sci Eng* **11**, 6 (2009)
28. J. Snoek, H. Larochelle, R.P. Adams, *Practical Bayesian optimization of machine learning algorithms* in Proc. NIPS (Lake Tahoe, Sierra Nevada, USA, 2012)
29. J. Snoek, K. Swersky, R. Zemel, R.P. Adams, in *NIPS Workshop on Bayesian Optimization in Theory and Practice*, (Lake Tahoe, Sierra Nevada, USA, 2013),
30. Z. Wang, N. deFreitas, University of Oxford, arXiv:1406.7758 (2014)
31. E. Brochu, V.M. Cora, N. de Freitas, *A Tutorial on Bayesian Optimization of Expensive Cost Functions, with Application to Active User Modeling and Hierarchical Reinforcement Learning* (Dept. of Computer Science, University of British Columbia, UBC TR-2009-23, 2009)
32. J.-A.M. Assael, Z. Wang, N. de Freitas, *Heteroscedastic Treed Bayesian Optimisation* in NIPS Workshop on Bayesian Optimisation (Montreal, Canada, 2014)
33. M.L.V. Ramires, C.A. Nieto De Castro, R.A. Perkins, Y. Nagasaka, A. Nagashima, M.J. Assael, W.A. Wakeham, *J. Phys. Chem. Ref. Data* **29**, 133 (2000)
34. Evaluation of Measurement Data - Guide to the Expression of Uncertainty in Measurement (GUM) (Joint Committee for Guides in Metrology, 2008)
35. R.W. Powell, C.Y. Ho, P.E. Liley, *Thermal Conductivity of Selected Materials, NSRDS-NBS 8* (National Bureau of Standards Reference Data Series, 1966)
36. D. Salmon, G. Roebben, A. Lamberty, R. Brandt, Certification of thermal conductivity and thermal diffusivity up to 1025K of a glass-ceramic reference material BCR-724, Report EUR 21764 EN, DG JRC (European Commission, Directorate-General, Joint Research Centre, Institute for Reference Materials and Measurements, 2007)
37. ASTM E438-92, *Standard Specification for Glasses in Laboratory Apparatus* (ASTM International, West Conshohocken, PA 2011)

38. I. Williams, R.E. Shawyer, Certification report for a pyrex glass reference material for thermal conductivity between -75 C and 195 C - CRM 039 (Community Bureau of Reference BCR, Commission of the European Communities, Brussels, 1991)
39. R.P. Tye, D.R. Salmon, Thermal Conductivity Reference Materials: Pyrex 7740 and Polymethyl Methacrylate, NPL Report (National Physical Laboratory, 2003)
40. S. Rudtsch, R. Stosch, U. Hammerschmidt, Intercomparison of measurements of the thermophysical properties of Crown Borosilicate Glass BK7 in European Conference on Thermophysical Properties (ECTP 2002) (London, GB, 2002)